Subramanyan Vasudevan[1]
Jothinathan Lakshmi[1]
Ganapathy Sozhan[1]

[1]Central Electrochemical Research Institute (CSIR), Karaikudi, India.

Research Article

Studies on the Removal of Iron from Drinking Water by Electrocoagulation – A Clean Process

The present study describes an electrocoagulation process for the removal of iron from drinking water using magnesium as the anode and galvanized iron as the cathode. Experiments were carried out as a function of pH, temperature and current density. The adsorption capacity was evaluated using both the Langmuir and the Freundlich isotherm models. The results show that the maximum removal efficiency of 98.4% was achieved at a current density of 0.06 A dm^{-2}, at a pH of 6.0. The adsorption of iron was better explained by fitting the Langmuir adsorption isotherm, which suggests a monolayer coverage of adsorbed molecules. The adsorption process followed a second-order kinetics model. Temperature studies showed that adsorption was endothermic and spontaneous in nature.

Keywords: Iron removal; Electrocoagulation; Clean technology; Adsorption kinetics; Isotherms

Received: August 21, 2008; *revised:* November 24, 2008; *accepted:* November 26, 2008

DOI: 10.1002/clen.200800175

1 Introduction

The presence of iron is probably the most common water problem faced by consumers and water professionals next to water hardness. Iron is commonly present in groundwater worldwide. In India, severe groundwater contamination by iron has been reported [1 – 4] by several states including Andhra Pradesh, Assam, Chhattisgarh, Karnataka and Orissa. Localized pockets are observed in states including Bihar, Jharkhand, Maharastra, Kerala, Madhya Pradesh, North Eastern States, Punjab, Rajasthan, Tamilnadu and Uttarpradesh. Although the presence of iron in the drinking water is not harmful to human health, it is undesirable. Bad taste, discoloration, staining and high turbidity are some of the aesthetic problems associated with iron content. Based on the above considerations, the World Health Organization (WHO) recommends that the iron contamination in drinking water should be less than 0.3 mg L^{-1} [5]. The European Commission directive recommends that the iron in water supplies should be less than 0.2 mg L^{-1} [6]. The Indian discharge limit for iron is 0.3 mg L^{-1} [7].

Iron usually exists in two oxidation states, reduced soluble divalent ferrous (Fe^{2+}) and oxidized trivalent ferric (Fe^{3+}). Several methods, e.g., oxidation-precipitation-filtration, lime softening, ion-exchange, activated carbon and other filtration materials, adsorption, bioremediation, supercritical fluid extraction, use of aerated granular filter, sub-surface iron removal and membrane processes have been employed for the removal of iron from groundwater [8 – 15]. The most commonly used methods for the removal of iron are oxidation-precipitation-filtration, ion exchange, lime softening and membrane processes. In the case of the ion exchange process, disadvantages including cost of resin, regeneration and waste disposal render the process uneconomical. Further, one of the major difficulties in using this method is that if any oxidation occurs during the process, then the resulting precipitate can coat and foul the ion exchange media. Oxidation followed by precipitation and filtration is a relatively simple process, but ineffective in the case of high iron concentrations, low pH and if the iron is complexed. The addition of lime causes the pH to rise up to 11 – 12. High maintenance costs and greater space requirements are the drawbacks of the process. The membrane process has emerged as a preferred alternative to provide safe drinking water. However, due to disadvantages such as high cost of membranes, brine disposal and post treatment of water, the process has also been proven to be uneconomical.

Recent research has demonstrated that electrochemistry offers an attractive alternative to the aforementioned traditional methods for treating wastewaters [16 – 22]. Electrochemical coagulation, which is one of these techniques, is the electrochemical production of destabilization agents that brings about charge neutralization for pollutant removal, and it has been widely used for water or wastewater treatment. Usually, aluminum, zinc or iron plates are used as electrodes in the electrocoagulation process. Electrochemically generated metallic ions from these electrodes can undergo hydrolysis near the anode to produce a series of activated intermediates that are able to destabilize the finely dispersed particles present in the water/wastewater to be treated. The destabilized particles then aggregate to form flocs as outlined below [23].

(i) When magnesium is used as the electrode, the reactions are as follows:

– At the cathode:

$$2\,H_2O + 2\,e^- \rightarrow H_2(g) + 2\,OH^- \quad (1)$$

– At the anode:

$$Mg \rightarrow Mg^{2+} + 2e^- \quad (2)$$

Correspondence: Dr. S. Vasudevan, Central Electrochemical Research Institute (CSIR), Karaikudi 630 006, India.
E-mail: vasudevan65@gmail.com

– In the solution:

$$Mg^{2+}(aq) + 2\,H_2O\,(l) \rightarrow Mg(OH)_2 + 2\,H^+(aq) \quad (3)$$

(ii) When aluminum is used as electrode, the reactions are as follows:
– At the cathode:

$$2\,H_2O + 2\,e^- \rightarrow H_2\,(g) + 2\,OH^- \quad (4)$$

– At the anode:

$$Al \rightarrow Al^{3+} + 3\,e^- \quad (5)$$

– In the solution:

$$Al^{3+}(aq) + 3\,H_2O \rightarrow Al(OH)_3 + 3\,H^+(aq) \quad (6)$$

The advantages of electrocoagulation include high particulate removal efficiency, a compact treatment facility, relatively low cost, and the possibility of complete automation. This method is characterized by reduced sludge production, a minimum requirement for chemicals, and ease of operation [24, 25]. Although there are numerous reports relating to electrochemical coagulation as a means of removal of many pollutants from water and wastewater, only limited work has been undertaken on iron removal by the electrochemical method and its adsorption and kinetics studies. This article presents the results of laboratory scale studies on the removal of iron using magnesium alloy and galvanized iron as the anode and the cathode, respectively, by an electrocoagulation process. In doing so, the equilibrium adsorption behavior is analyzed by fitting Langmuir and Freundlich isotherm models. The adsorption kinetics of the electrocoagulants are analyzed using first- and second-order kinetic models. Finally, the activation energy is evaluated to study the nature of the adsorption.

2 Experimental

2.1 Cell Construction and Electrolysis

The electrolytic cell is shown in Fig. 1 and consists of a 1.0 L Plexiglas vessel that was fitted with a polyvinylchloride (PVC) cell cover with slots to introduce the electrodes, pH sensor, a thermometer and the electrolytes. Magnesium (Alfa Aesar) with a surface area of 0.02 m^2 acted as the anode. The cathode was a galvanized iron (commercial grade) sheet of the same size as the anode and was placed at an inter-electrode distance of 0.005 m. The temperature of the electrolyte was controlled to the desired value with a variation of ±2 K by adjusting the rate of flow of thermostatically controlled water through an external glass-cooling spiral. A regulated direct current was supplied from a rectifier (10 A, 0–25 V, Aplab model).

The iron ($FeSO_4$, Analar Reagent) was dissolved in tap (drinking) water to give the required concentration. 0.90 L of solution was used as the electrolyte for each experiment. The pH of the electrolyte was adjusted, if required, with 1 M HCl or 1 M NaOH solutions before adsorption experiments were undertaken.

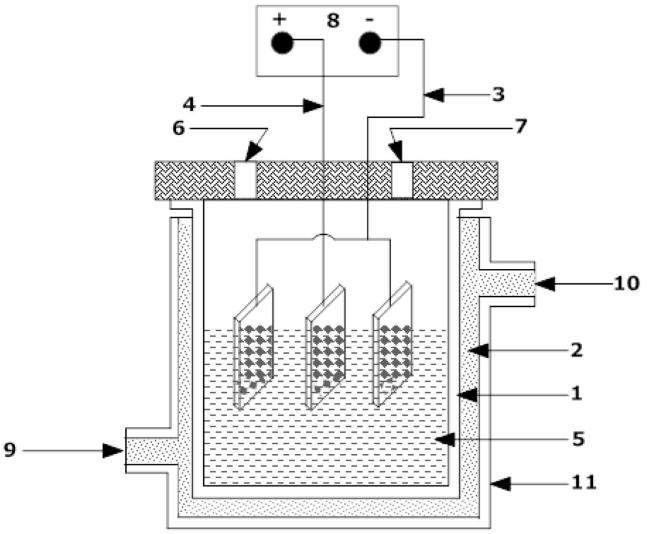

Figure 1. Laboratory scale cell assembly: (1) Cell, (2) Thermostatic water, (3) Galvanized iron cathode, (4) Anode, (5) Electrolyte, (6) and (7) Holes to introduce pH sensor and thermometer, (8) DC source, (9) Inlet of thermostatic water, (10) Outlet of thermostatic water, and (11) Thermostat.

2.2 Analysis

The concentration of iron was determined using an atomic absorption spectrophotometer made by Varian, The Netherlands and Spectro Quant analysis, Merck. The surface morphology of the anode, both before and after treatment, was analyzed with a metallurgical microscope made by ZEISS, Germany.

3 Results and Discussion

3.1 Effect of Current Density

Current density is the one of the most important operational parameters in elecrocoagulation processes. To investigate the effects of current density, a series of experiments were carried out using 25 mg L^{-1} iron-containing solutions, at pH 6.0, with the current density being varied from 0.02 to 0.12 A dm^{-2}. The removal efficiency of iron increases rapidly up to 98.4% with a current density of 0.06 A dm^{-2} and then it remains almost constant for higher current densities as shown in Fig. 2. According to Faraday's law, the current density is directly proportional to the amount of adsorbent (magnesium hydroxide) formed, which is related to the time and current density. Hence, the amount of iron adsorption increases with the increase in adsorbent concentration, which indicates that the adsorption depends on the availability of binding sites for iron.

3.2 Effect of pH

It has been established that the pH of the electrolyte is one of the important factors affecting the performance of an electrochemical process, and that it has a particularly strong effect on the performance of an electrocoagulation process. To evaluate its effect, a series of experiments were performed, using 25 mg L^{-1} of iron-containing solution with an initial pH varying in the range 4–9. As illustrated

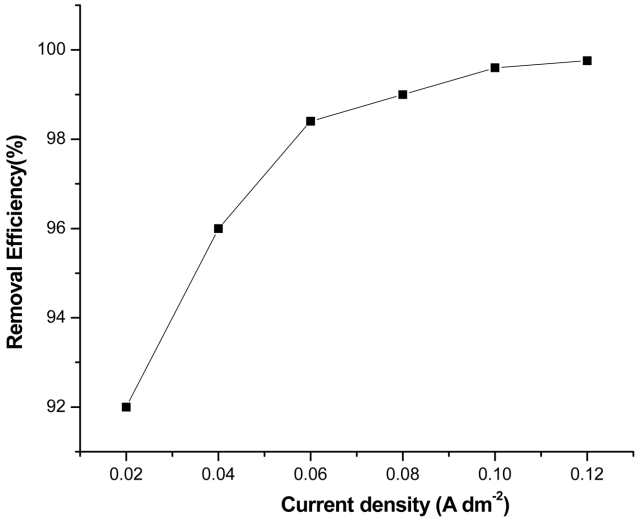

Figure 2. Effect of current density on the removal of iron. Conditions are solution pH: 6.0, concentration of iron: 25 mg L^{-1}, and solution temperature: 305 K.

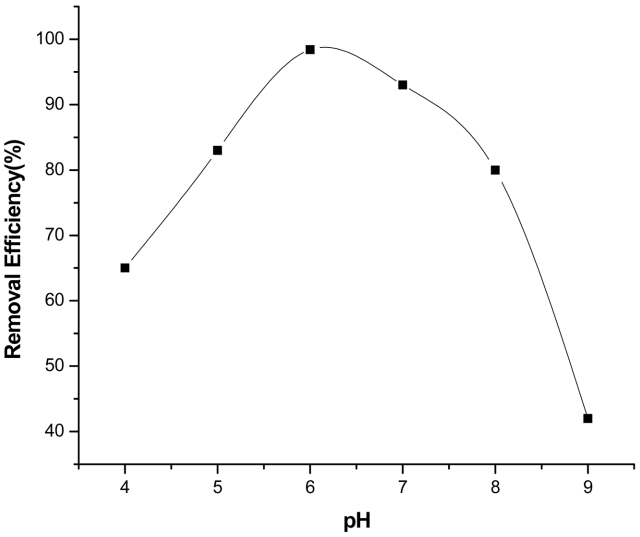

Figure 3. Effect of pH on the removal of iron. Conditions are concentration of iron: 25 mg L^{-1}, current density: 0.06 A dm^{-2}, and solution temperature: 305 K.

in Fig. 3, it can be seen that the removal efficiency of iron increased with increasing pH and that a maximum removal efficiency of 98.4% was obtained at pH 6.0.

A decrease of removal efficiency at more acidic and alkaline pH values was observed by many investigators [26] and was attributed to the amphoteric behavior of $Al(OH)_3$, which leads to soluble Al^{3+} cations (at acidic pH) and to monomeric anions $Al(OH)^{4-}$ (at alkaline pH). It is well known that these soluble species are not useful for water treatment. When the initial pH was maintained at neutral, all of the aluminium produced at the anode formed polymeric species ($Al_{13}O_4(OH)_{24}^{7+}$) and precipitated $Al(OH)_3$ leading to greater removal efficiency [26]. In the present study, the electrolyte pH was maintained at neutral, so that the formation of $Mg(OH)_2$ is more predominant (like aluminium), leading to a greater removal efficiency.

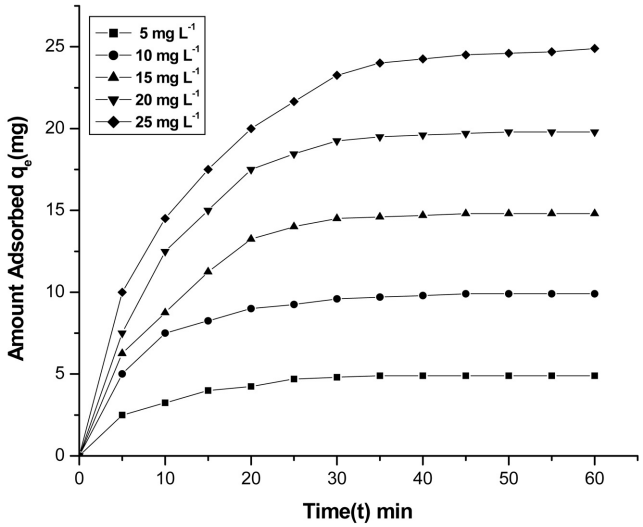

Figure 4. Effect of agitation time and initial iron concentration on the amount of iron adsorbed. Conditions are solution pH: 6.0, solution temperature: 305 K, and current density: 0.06A dm^{-2}.

3.3 Effect of Initial Iron Concentration

The adsorption of iron (ferrous) is increased with an increase in iron concentration and remains constant after the equilibrium time is reached, as depicted in Fig. 4. The equilibrium time was 35 min for all of the concentrations studied (5 – 25 mg L^{-1}). The amount of iron adsorbed, q_e, increased from 5.437 to 29.45 mg g^{-1} of $Mg(OH)_2$, as the concentration was increased from 5 to 25 mg L^{-1}. It is also clear from Fig. 4 that the adsorption is rapid in the initial stages and gradually decreases with progress of adsorption. The plots are single, smooth, and continuous curves leading to saturation, suggesting the possible monolayer coverage of iron on the surface of the adsorbent [27].

3.4 Adsorption Kinetics

The adsorption kinetic data of iron are analyzed using the Lagergran rate equation [28, 29]. The integrated form of the Lagergran equation with the boundary conditions of $t = 0$ to $t = t$ and $q_t = 0$ to $q_t = q_t$ can be written as given in Eq. (7):

$$\log (q_e - q_t) = \log q_e - k_1 t/2.303 \quad (7)$$

where q_t and q_e are the amount of iron adsorbed (mg) at time t (min) and at equilibrium time, respectively, and k_1 (min^{-1}) is the rate constant of first-order adsorption. The values of q_e and the rate constant k_1 were calculated from the slope of the plots of log ($q_e - q_t$) versus time t. Linear plots of log ($q_e - q_t$) vs t indicate the applicability of the above equation. It was found that the calculated q_e values do not agree with the experimental values. Therefore, the kinetics of iron adsorption on magnesium hydroxide does not follow a first-order rate expression [30].

The second-order kinetic model is expressed as Eq. (8) [31]:

$$t/q_t = 1/k_2 q_e^2 + t/q_e \quad (8)$$

The plot of t/q_t versus time t given in Fig. 5 shows a straight line. The second-order kinetic values of q_e and k_2 were calculated from

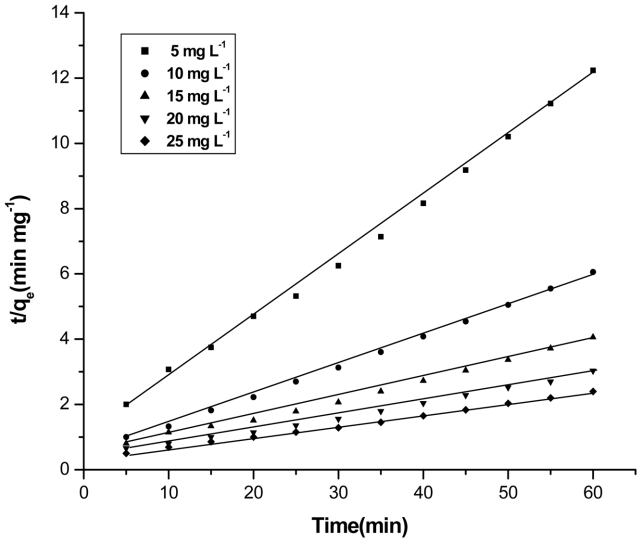

Figure 5. Second-order kinetic model plot for different concentrations of iron. Conditions are solution pH: 6.0, solution temperature: 305 K, and current density: 0.06A dm^{-2}.

Table 1. Comparison between the experimental and calculated q_e values for different initial iron concentrations in a second-order adsorption isotherm at a temperature of 305 K and pH 6.0.

Concentration of Iron [mg L^{-1}]	Experimental q_e [mg g^{-1}]	k_2 [min g mg^{-1}]	Calculated q_e [mg g^{-1}]	R^2
5	4.9	0.0352	4.731	0.9984
10	9.7	0.0256	9.607	0.9997
15	14.6	0.0067	17.47	0.9938
20	19.5	0.0053	18.79	0.9962
25	24.0	0.0036	23.23	0.9986

Table 2. Comparison between the experimental and calculated q_e values for an initial iron concentration of 25 mg L^{-1} in a second-order adsorption isotherm at various temperatures and pH 6.0.

Temperature [K]	Experimental q_e [mg g^{-1}]	k_2 [min g mg^{-1}]	Calculated q_e [mg g^{-1}]	R^2
303	24	0.00362	23.23	0.99868
313	24.60	0.00573	23.98	0.9994
323	24.7	0.0104	24.28	0.99896
333	24.9	0.0163	24.50	0.994

the slope and intercept of the plots of t/q_t versus t. The plot shows that the correlation coefficients for the second-order kinetic model obtained in all of the concentration studies were above 0.99, and also the calculated q_e values agree with the experimental q_e values. Table 1 depicts the computed result obtained from the second-order kinetic model. These results indicate that the adsorption system studied obeys second-order kinetics. Similar phenomena have been observed in the adsorption of phosphate in Fe (III)/Cr (III) hydroxide [27].

Using the Lagergran rate equation, first-order rate constants and correlation coefficients were calculated for different temperatures, i.e., 303 to 333 K. The calculated 'q_e' values obtained from the first-order kinetics do not agree with the experimental 'q_e' values. The second-order kinetics model shows that the calculated 'q_e' values agree with the experimental values, Tab. 2. This indicates that the adsorption follows the second-order kinetic model at the different temperatures used in this study. From the table, it is found that the rate constant, k_2, increased on increasing the temperature from 305 to 333 K. The increase in adsorption may be due to a change in pore size on increasing the kinetic energy of the iron species and resulting in an enhanced rate of intraparticle diffusion of the adsorbate.

3.5 Adsorption Isotherm

The adsorption capacity of the adsorbent was tested using Freundlich [32] and Langmuir [33] isotherms. To determine the isotherms, the initial pH was kept at 6.0 and the concentration of iron used was in the range of 5 to 25 mg L^{-1}. The general form of Freundlich adsorption isotherm is represented by Eq. (9) [32]:

$$q_e = KC^n \tag{9}$$

Eq. (9) can be linearized in logarithmic form, and the Freundlich constants can be determined as follows, Eq. (10):

$$\log q_e = \log k_f + 1/n \log C_e \tag{10}$$

where k_f is the Freundlich constant related to adsorption capacity, n is the energy or intensity of adsorption, and C_e is the equilibrium concentration of the iron (mg L^{-1}). The Freundlich constants, k_f, and n values are 0.993 mg/g and 1.008 L/mg, respectively. It has been reported that values of n lying between 1 and 10 indicate favorable adsorption [27]. From the analysis of the results, it is found that the Freundlich plots satisfactorily fit the experimental data obtained in the present study. This agrees well with the results presented in the literature [27].

The Langmuir isotherm has been used to study the surface monolayer adsorption with uniform energies of adsorption on the surface and to show that there is no transmigration of adsorbate in the plane of the surface. The Langmuir isotherm can be expressed as Eq. (11) [33]:

$$C_e/q_e = 1/q_o b + C_e/q_o \tag{11}$$

where C_e is the concentration of the iron solution (mg L^{-1}) at equilibrium, q_o is the maximum capacity to form a complete monolayer on the surface, and b is the Langmuir constant related to the free energy of adsorption. The Langmuir plot is a better fit with the experimental data compared to the Freundlich plots. The value of the adsorption capacity, q_o, was found to be 1311.47 mg/g, which is higher than that of other adsorbents studied [29].

The essential characteristics of the Langmuir isotherm can be expressed in terms of a dimensionless constant separation factor or equilibrium parameter, R_L which is defined by [34]:

$$R_L = 1/(1 + bC_o) \tag{12}$$

where R_L is the equilibrium parameter, C_o is the initial iron concentration and b is the Langmuir constant. The R_L values indicate the type of isotherm: for irreversible reactions ($R_L = 0$), favorable ($0 < R_L < 1$), linear ($R_L = 1$) or unfavorable ($R_L > 1$) [35]. In present study, the R_L values were found to be between 0 and 1 for the concentration range of iron studied (5–25 mg L^{-1}). The results are presented in Tab. 3.

Table 3. Langmuir constants for the adsorption of iron at a tenmperature of 305 K and pH 6.0.

Concentration of Iron [mg L^{-1}]	q_m [mg]	K_a [L mg^{-1}]	R_L
5	–	–	0.9643
10	–	–	0.9310
15	1311.47	0.000749	0.8994
20	–	–	0.8703
25	–	–	0.8423

Table 4. Pore diffusion coefficients for the adsorption of iron at different concentrations and temperature at pH 6.0.

Concentration of Iron [mg L^{-1}]	Pore Diffusion Constant, $D \cdot 10^9$ [cm^2 s^{-1}]
5	3.6
10	3.6
15	3.0
20	2.25
25	2.088
Temperature [K]	**Pore Diffusion Constant, $D \cdot 10^9$ [cm^2 s^{-1}]**
303	2.088
313	3.6
323	4.32
333	5.04

3.6 Effect of Temperature

The adsorption of iron increases with the increase in temperature showing that the process is endothermic [36]. The diffusion coefficient, D, for the intraparticle transport of an iron species into the adsorbent particles has been calculated at different temperatures by Eq. (13):

$$t_{1/2} = 0.03\ (r_o^2/D) \tag{13}$$

where $t_{1/2}$ is the time of half adsorption (s), r_o is the radius of the adsorbent particle (cm), and D is the diffusion coefficient in $cm^2\ s^{-1}$. In the present work, D is found to be in the range of 10^{-9} $cm^2 s^{-1}$. For all chemisorption systems, the diffusivity coefficient should be 10^{-5} to 10^{-13} $cm^2 s^{-1}$ [37]. The values of the pore diffusion coefficient, D, are presented in Tab. 4 for different initial concentrations of iron and temperature and it is found that the system in the present study follows the chemisorption system.

In order to determine the energy of activation for the adsorption of iron, the second-order rate constant is expressed in the Arrhenius form, Eq. (14) [38]:

$$\log k_2 = \log k_0 - \frac{E}{2.303\,RT} \tag{14}$$

where k_o is the constant of the equation (g min/mg), E is the energy of activation (J/mol), R is the gas constant (8.314 J $mol^{-1} K^{-1}$), and T is the temperature in K. The activation energy (18.416 kJ mol^{-1}) is calculated from the slope ($\log K_2$ vs T^{-1}) of the fitted equation. The thermodynamic parameters such as free energy change, ΔG^0, enthalpy change, ΔH^0, and entropy change, ΔS^0, have been calculated using the following relationships, Eq. (15):

$$\Delta G^0 = -RT \ln K_c \tag{15}$$

Table 5. Thermodynamic parameters for the adsorption of iron.

Temperature [K]	ΔG^0 [J mol^{-1}]	ΔH^0 [kJ mol^{-1}]	ΔS^0 [J $mol^{-1} K^{-1}$]
303	−184.14	–	–
313	−797.8	18.234	60.75
323	−1411.72	–	–
333	−2025.75	–	–

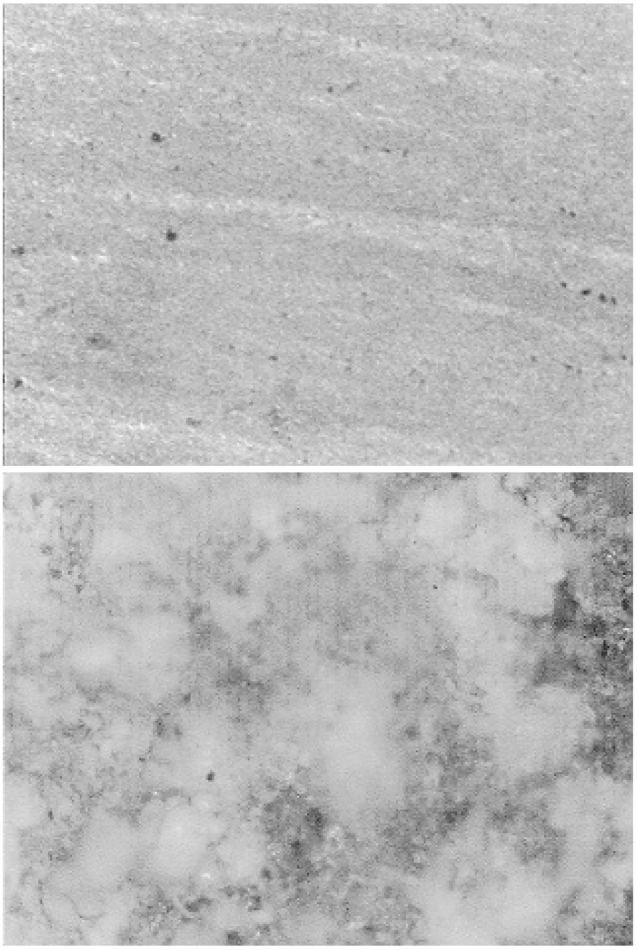

Figure 6 Microscopic image of the anode (a) Before, and (b) After treatment.

where ΔG^0 is the change in free energy (kJ mol^{-1}), K_c is the equilibrium constant, R is the gas constant and T is the temperature in K. The ΔG^0 values are presented in Tab. 5. From the table it is found that the negative value of ΔG^0 indicates the spontaneous nature of adsorption.

Other thermodynamic parameters such as entropy change, ΔS^0, and enthalpy change, ΔH^0, were determined using the van't Hoff expression, Eq. (16):

$$\log K_c = \frac{\Delta S^0}{2.303\,R} - \frac{\Delta H^0}{2.303\,RT} \tag{16}$$

The enthalpy change, ΔH^0, and entropy change, ΔS^0, were obtained from the slope and intercept of the van't Hoff linear plots of ln K_c versus $1/T$. A positive value of enthalpy change, ΔH^0, indi-

cates that the adsorption process is endothermic in nature, and the negative value of change in free energy, ΔG^0, shows the spontaneous adsorption of iron on the adsorbent. The positive values of entropy change show the increased randomness of the solution interface during the adsorption of iron on the adsorbent, see Tab. 5. The enhancement of the adsorption capacity of the electrocoagulant (magnesium hydroxide) at higher temperatures may be attributed to the enlargement of the pore size and/or activation of the adsorbent surface.

Figures 6a) and 6b) show microscopic images of the anode, before and after, treatment. The microscopic image indicates the presence of micron-sized particles on the surface.

4 Conclusions

The results of this work showed that a removal efficiency of 98.4% was achieved at an optimum current density of 0.06 A dm^{-2} and a pH of 6.0 using magnesium as the anode and galvanized iron as the cathode. The magnesium hydroxide generated in the cell removed the iron present in the water and reduced the iron concentration to 0.1 to 0.3 mg L^{-1}, making it drinkable. The results indicate that the process can be scaled up to higher capacities. The adsorption of iron appears to have a preferential fit to the Langmuir adsorption isotherm, which suggests monolayer coverage of adsorbed molecules. The adsorption process follows second-order kinetics. Temperature studies showed that adsorption was endothermic and spontaneous in nature.

Acknowledgements

The authors wish to express their gratitude to the Director, Central Electrochemical Research Institute, Karaikudi, for assistance in publishing this article.

The authors have declared no conflict of interest.

References

[1] B. Das, et al., Fluoride and other inorganic constituents in groundwater of Guwahati, Assam, India, *Curr. Sci.* **2003**, *85 (5)*, 657.

[2] D. B. Mahanta, N. N. Das, R. K. Dutta, A chemical and bacteriological study of drinking water in tea gardens of central Assam, *Indian J. Environ. Prot.* **2004**, *24 (5)*, 654.

[3] R. Sharma, S. Shah, C. Mahanta, Hydrogeochemical study of groundwater fluoride contamination: a case study from Guwahati city, India, *Asian J. Water Environ. Pollut.* **2005**, *2 (1)*, 47.

[4] N. Subba Rao, Iron content in groundwaters of Visakhapatnam environs, Andhra Pradesh, India, *Environ. Monit. Assess.* **2008**, *136 (1 – 3)*, 437.

[5] *WHO Guidelines for Drinking Water Quality: Health Criteria and Other Supporting Information*, 2nd ed., WHO, Geneva **1996**.

[6] Council Directive 98/83/EC on the Quality of Water Intended for Human Consumption, *Off. J. Eur. Commun.* **1998**, L330/32 – L330/50.

[7] *Central Pollution Control Board, Ministry of Environment and Forests*, Govt. of India, Delhi **2008**. (www.cpcb.nic.in).

[8] K. Vaaramaa, J. Lehto, Removal of metals and anions from drinking water by ion exchange, *Desalination* **2003**, *155 (2)*, 157.

[9] R. Munter, H. Ojaste, J. Sutt, Complexed iron removal from groundwater, *J. Environ. Eng.* **2005**, *131 (7)*, 1014.

[10] W. C. Andersen, T. J. Bruno, Application of gas-liquid entraining rotor to supercritical fluid extraction: removal of iron (III) from water, *Anal. Chim. Acta* **2003**, *485 (1)*, 1.

[11] P. Berbenni et al., Removal of iron and manganese from hydrocarbon-contaminated groundwaters, *Bioresour. Technol.* **2000**, *74 (2)*, 109.

[12] H. A. Aziz et al., Physicochemical removal of iron from semiaerobic landfill leachate by limestone filtration, *Water Manage.* **2004**, *24 (4)*, 353.

[13] D. Ellis, C. Bouchard, G. Lantagne, Removal of iron and manganese from groundwater by oxidation and microfiltration, *Desalination* **2000**, *130 (3)*, 255.

[14] B. Das et al., Removal of iron by groundwater by ash: a systematic study of a traditional method, *J. Hazard. Mater.* **2007**, *141 (3)*, 834.

[15] B. Y. Cho, Iron removal using aerated granular filter, *Process Biochem.* **2005**, *40 (10)*, 3314.

[16] D. W. Miwa, G. R. P. Malpass, S. A. S. Machado, A. J. Motheo, Electrochemical degradation of carbaryl on oxide electrodes, *Water Res.* **2006**, *40 (17)*, 3281.

[17] E. Onder, A. S. Koparal, U. B. Ogutveren, An alternative method for the removal of surfactants from water: Electrochemical coagulation, *Sep. Purif. Technol.* **2007**, *52 (3)*, 527.

[18] M. Ikematsu, K. Kaneda, M. Iseki, M. Yasuda, Electrochemical treatment of human urine for its storage and reuse as flush water, *Sci. Total Environ.* **2007**, *382 (2 – 3)* 159.

[19] C. Carlesi Jara et al., Electrochemical removal of antibiotics from wastewaters, *Appl. Catal., B* **2007**, *70 (1 – 4)*, 479.

[20] P. A. Christensen et al., A novel electrochemical device for the disinfection of fluids by OH radicals, *Chem. Commun.* **2006**, *38*, 4022.

[21] A. Carlos, M. Huitle, S. Ferro, Electrochemical oxidation of organic pollutants for the wastewater treatment: direct and indirect processes, *Chem. Soc. Rev.* **2006**, *35 (12)*, 1324.

[22] C. Gabrielli et al., Electrochemical water softening: principle and application, *Desalination* **2006**, *201 (1 – 3)*, 150.

[23] X. Chen, G. Chen, P. L. Yue, Investigation on the electrolysis voltage of electrocoagulation, *Chem. Eng. Sci.* **2002**, *57 (23)*, 2449.

[24] G. Chen, Electrochemical technologies in wastewater treatment, *Sep. Purif. Technol.* **2004**, *38 (1)*, 11.

[25] N. Adhoum, L. Monser, Decolorization and removal of phenolic compounds from olive mill wastewater by electrocoagulation, *Chem. Eng. Process.* **2004**, *43 (8)*, 1281.

[26] M. Kobya, O. T. Can, M. Bayramoglu, Treatment of textile wastewaters by electrocoagulation using iron and aluminium electrodes, *J. Hazard. Mater.* **2003**, *B100 (1 – 3)*, 163.

[27] C. Namasivayam, K. Prathap, Recycling Fe (III)/Cr (III) hydroxide, an industrial solid waste for the removal of phosphate from water, *J. Hazard. Mater.* **2005**, *123B (1 – 3)*, 127.

[28] G. Bina, I. Begum Zareena, R. Garima, Equilibrium and kinetic studies for the Adsorption of Mn(II) and Co (II) from aqueous media using agar-agar adsorbent, *Res. J. Chem. Environ.* **2007**, *11 (3)*, 16.

[29] G. Mckay, Y. S. Ho, The sorption of lead (II) on peat, *Water Res.* **1999**, *33 (2)*, 578.

[30] C. Namasivayam, S. SenthilKumar, Recycling of industrial solid waste for the removal of mercury (II) by adsorption process, *Chemosphere* **1997**, *34 (2)*, 357.

[31] C. Namasivayam, S. Senthil Kumar, Removal of arsenic (V) from aqueous solutions using industrial solid waste: Adsorption rates and equilibrium studies, *Ind. Eng. Chem. Res.* **1998**, *37 (12)*, 4816.

[32] H. Freundlich, Uber, Die adsorption in losungen, *Z. Phys. Chem. (Muenchen, Germany)* **1985**, *57 (3)*, 387.

[33] I. Langmuir, The adsorption of gases on plane surface of gases on plane surface of glass, mica and platinum, *J. Am. Chem. Soc.* **1918**, *40 (1)*, 1361.

[34] L. D. Michelson, P. G. Gideon, E. G. Pace, L. H. Kutal, Removal of solute mercury from wastewater by a complexing technique, *US Department of Industry*, *Office of Water Research and Technology Bulletin*, Washington DC **1975**.

[35] W. Nigussie, F. Zewgeb, B. S. Chandravanshi, Removal of excess fluoride from water using waste residue from alum manufacturing process, *J. Hazard. Mater.* **2007**, *147 (3)*, 954.

[36] S. Nayak Preeti, B. K. Singh, Sorption dynamics of phenol on naturally occurring low cost clay, *Res. J. Chem. Environ.* **2007**, *11 (1)*, 23.

[37] X.-Y. Yang, B. Al-Duri, Application of branched pore diffusion model in the adsorption of reactive dyes on activated carbon, *Chem. Eng. J.* **2001**, *83 (1)*, 15.

[38] A. K. Golder, A. N. Samantha, S. Ray, Removal of phosphate from aqueous solution using calcined metal hydroxides sludge waste generated from electrocoagulation, *Sep. Purif. Technol.* **2006**, *52(1)*, 102.

